An Adaptive Neurofuzzy Approach for the Diagnosis in Wireless Capsule Endoscopy Imaging

V. S. Kodogiannis[1], M. Boulougoura[2]

[1]Centre for Systems Analysis, School of Computer Science,
Univ. of Westminster, London, HA1 3TP, U.K
V.Kodogiannis@westminster.ac.uk
[2]IBM Hellas S.A., Athens, GR-15232, Greece

Abstract

Computerised processing of medical images can ease the search of the representative features in the images. The endoscopic images possess rich information expressed by texture. In this paper schemes have been developed to extract new texture features from the texture spectra in the chromatic and achromatic domains for a selected region of interest from each colour component histogram of images acquired by the new M2A Swallowable Capsule. The implementation of a neurofuzzy scheme and the concept of fusion of multiple classifiers have been also adopted in this paper. The preliminary test results support the feasibility of the proposed method.

Keyword: Medical imaging, Computer aided diagnosis, Endoscopy, Neuro-fuzzy networks, Fuzzy integral.

I. Introduction

Medical diagnosis is based on information obtained from various sources, such as results of clinical examinations and histological findings, patients' history and other data that physician considers in order to reach a final diagnostic decision [1]. Imaging techniques have been extensively used, in the last decades, as a valuable tool in the hands of an expert for a more accurate judgment of patients' condition. Since the beginning of computer technology, it becomes necessary for visual systems to "understand a scene", that is making its own properties to be outstanding, by enclosing them in a general description of an analysed environment. Computer-assisted image analysis can extract the representative features of the images together with quantitative measurements and thus can ease the task of objective interpretations by a physician expert in endoscopy.

Krishnan, *et al.* [2] has been using endoscopic images to define features of the normal and the abnormal colon. New approaches for the characterisation of colon based on a set of quantitative parameters, extracted by the fuzzy processing of colon images, have been used for assisting the colonoscopist in the assessment of the status of patients and were used as inputs to a rule-based decision strategy to find out whether the colon's lumen belongs to either an abnormal or normal category. The quantitative characteristics of the colon are: mean and standard deviation of RGB, perimeter, enclosed boundary area, form factor, and centre of mass. The analysis of the extracted quantitative parameters was performed using three different neural networks selected for classification of the colon. The three networks include a two-layer perceptron trained with the delta rule, a multilayer perceptron with back-propagation (BP) learning and a self-organizing network. A comparative study of the three methods was also performed and it was observed that the self-organizing network is more appropriate for the classification of colon status. Endoscopic images contain rich information of texture. Therefore, the additional texture information can provide better results for the image analysis than approaches using merely intensity information. Such information has been used in CoLD (colorectal lesions detector) an innovative detection system to support colorectal cancer diagnosis and detection of pre-cancerous polyps, by processing endoscopy images or video frame sequences acquired during colonoscopy [3]. It utilised second-order statistical features that were calculated on the wavelet transformation of each image to discriminate amongst regions of normal or abnormal tissue. A neural network based on the classic BP learning algorithm performed the classification of the features. CoLD integrated the feature extraction and classification algorithms under a graphical user interface, which allowed both novice and expert users to utilise effectively all system’s functions. The detection accuracy of the proposed system has been estimated to be more than 95%.

Recently a new wireless endoscopy system has been developed by Israeli-based Given Imaging Limited and produces high-quality images of the small bowel without pain or discomfort to the patient [4]. The system consists of a small swallowable capsule containing a battery, a camera on a chip, a light source, and a transmitter as shown in Fig. 1. The camera-capsule has a length of three centimetres so it can be swallowed with some effort. In 24 hours, the capsule is crossing the patient's alimentary canal. For the purpose of this research work, endoscopic images have been obtained using this innovative endoscopic device. They have spatial resolution of 171x151 pixels, a brightness resolution of 256 levels per colour plane (8bits), and consisted of three colour planes (red, green and blue) for a total of 24 bits per pixel. The proposed methodology in this paper is considered in two phases.

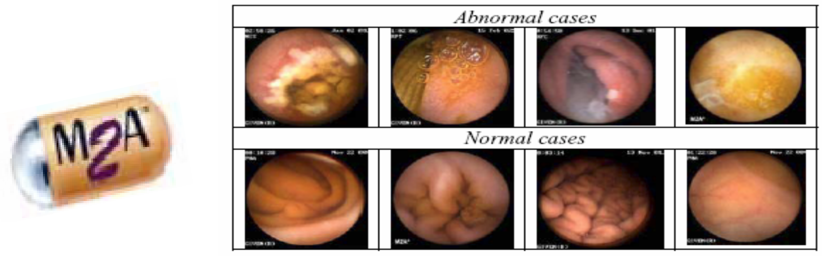

Fig. 1: Selected endoscopic images of normal and abnormal cases

The first implements the extraction of image features while in the second phase one neurofuzzy scheme is implemented / employed to perform the diagnostic task. In this research, a new approach of obtaining statistical features/parameters from the texture spectra is proposed both in the chromatic and achromatic domains of the image. The definition of texture spectrum employs the determination of the texture unit (*TU*) and texture unit number (N_{TU}) values. Texture units characterise the local texture information for a given pixel and its neighbourhood, and the statistics of the entire texture unit over the whole image reveal the global texture aspects. For the diagnostic part, the concept of multiple-classifier scheme has been adopted, where the fusion of the individual outputs was realised using fuzzy integral. The neurofuzzy classifier-scheme adopted in this study utilises a defuzzification method, namely area of balance (AOB).

II. Image Features Extraction

A major component in analysing images involves data reduction which is accomplished by intelligently modifying the image from the lowest level of pixel data into higher level representations. Texture is broadly defined as the rate and direction of change of the chromatic properties of the image, and could be subjectively described as fine, coarse, smooth, random, rippled, and irregular, etc. The analysis of texture in object images is a very important area of research as new algorithms are continuously being sought that can improve our ability to characterise objects of different types with unique feature signatures. This methodology is better developed in the case of grey-scale image analysis as opposed to colour image analysis. In general, there are three main approaches to combine colour and texture: parallel, sequential, and integrative [13]. In the parallel approach, colour and texture are evaluated separately. Sequential approaches use colour analysis as a first step of the process chain: After the colour space is quantised, grey-scale texture methods are applied. The integrative method uses the different colour channels of an image and performs the grey-scale texture analysis methods on each channel separately. Similar to texture, colour is one of the most important features of objects in image and video data. Each pixel in an image has a three-dimensional colour vector and different colour space approaches exist to represent colour information. One of these colour space models is the hardware-oriented Red-Green-Blue Model (RGB), where the colour vector of a pixel *p* is the compound of red, green and blue channels. Another colour space model is the Hue-Saturation-Intensity Value Model (HSV) that is based on colour descriptions rather than individual colour components. The RGB model has a major drawback: it is not perceptually uniform. Therefore, most of the systems use colour space models other than RGB, such as HSV. The HSV colour space is particularly useful because it is closer to the human perception of colours. Hue refers to the dominant wavelength of the colour, while saturation depicts the mount of whiteness in the colour. Value describes the brightest intensity among the red, green and blue images on the same pixel.

For the current research work the integrative methodology has been adopted, using the RGB and HSV colour channels for the extraction of colour texture information. We exploited the HSV colour space, because the lesions present marked differences, especially for the saturation image. The HSV colour space can be derived through a transformation of the RGB space.

We thus focused our attention on nine statistical measures (standard deviation, variance, skew, kurtosis, entropy, energy, inverse difference moment, contrast, and covariance). All texture descriptors are estimated for all planes in both RGB {R (Red), G (Green), B (Blue)} and HSV {H (Hue), S (Saturation), V (Value of Intensity)} spaces, creating a feature vector for each descriptor $D_i=(R_i,G_i,B_i,H_i,S_i,V_i)$ [6]. Thus, a total of 54 features (9 statistical measures x 6 image planes) are then estimated. For our experiments, we have used 70 endoscopic images related to abnormal cases and 70 images related to normal ones. Fig. 1 shows samples of selected images acquired using the M2A capsule of normal and abnormal cases. Generally, the statistical measures are estimated on histograms of the original image (1st order statistics) [5]. However, the histogram of the original image carries no information regarding relative position of the pixels in the texture. Obviously this can fail to distinguish between textures with similar distributions of grey levels. We therefore have to implement methods which recognise characteristic relative positions of pixels of given intensity levels. An alternative scheme is proposed in this study to extract new texture features from the texture spectra in the chromatic and achromatic domains, for a selected region of interest from each colour component histogram of the endoscopic images.

A. N_{TU} Transformation

The definition of texture spectrum employs the determination of the texture unit (*TU*) and texture unit number (N_{TU}) values. Texture unit may be considered as the smallest complete unit which best characterises the local texture aspect of a given pixel and its neighbourhood in all eight directions of a square raster. In a square raster digital image each pixel is surrounded by eight neighbouring pixels. The local texture information for a pixel can be extracted from a neighbourhood of 3x3 pixels, which represents the smallest complete unit (in the sense of having eight directions surrounding the pixel). Texture units thus characterise the local texture information for a given pixel and its neighbourhood, and the statistics of all the texture units over the whole image reveal the global texture aspects. Given a neighbourhood of $\delta \times \delta$ pixels, which are denoted by a set containing $\delta \times \delta$ elements $P = \{P_0, P_1, ..., P_{(\delta\times\delta)-1}\}$, where P_0 represents the chromatic or achromatic (i.e. intensity) value of the central pixel and P_i $\{i = 1, 2, ..., (\delta \times \delta) - 1\}$ is the chromatic or achromatic value of the neighbouring pixel i , the $TU = \{E_0, E_1, ..., E_{(\delta\times\delta)-1}\}$, where $E_i \{i = 1, 2, ..., (\delta\times\delta) - 1\}$ is determined as follows:

$$E_i = \begin{cases} 0, & if \quad P_i < P_0 \\ 1, & if \quad P_i = P_0 \\ 2, & if \quad P_i > P_0 \end{cases} \tag{1}$$

The element E_i occupies the same position as the i^{th} pixel. Each element of the *TU* has one of three possible values; therefore the combination of all the eight elements results in 6561 possible *TU*'s in total.

a	b	c
h		d
g	f	e

Fig 2: Eight clockwise, successive ordering ways of the eight elements of the texture unit. The first element E_i may take eight possible positions from *a* to *h*

The texture unit number (N_{TU}) is the label of the texture unit and is defined using the following equation:

$$N_{TU} = \sum_{i=1}^{(\delta\times\delta)-1} E_i \times \delta^{i-1} \tag{2}$$

Where, in our case, $\delta = 3$

In addition, the eight elements may be ordered differently. If the eight elements are ordered clockwise as shown in Fig. 2, the first element may take eight possible positions from the top left (*a*) to the middle left (*h*), and then the 6561 texture units can be labelled by the Eq. 1, under eight different ordering ways (from *a* to *h*). Fig. 3 provides an example of transforming a neighbourhood to a texture unit with the texture unit number under the ordering way *a* [11].

The previously defined set of 6561 texture units describes the local-texture aspect of a given pixel; that is, the relative grey-level relationships between the central pixel and its neighbour. Thus the statistics of the frequency of occurrence of all the texture units over a large region of an image should reveal texture information. The texture spectrum histogram (*Hist*(*i*)) is obtained as the frequency distribution of all the texture units, with the abscissa showing the N_{TU} and the ordinate representing its occurrence frequency.

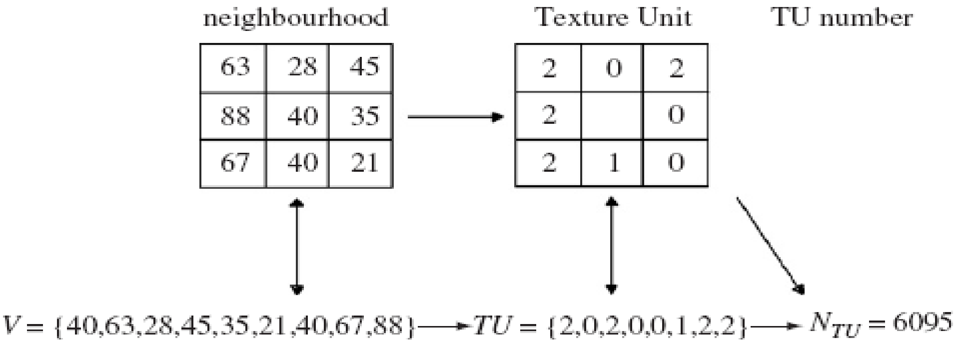

Fig.3: Example of transforming a neighbourhood to a texture unit with the texture-unit number

The texture spectra of various image components {V (Value of Intensity), R (Red), G (Green), B (Blue), H (Hue), S (Saturation)} are obtained from their texture unit numbers. The statistical features are then estimated on the histograms of the N_{TU} transformations of the chromatic and achromatic planes of the image (R,G,B,H,S,V).

III. Image Features Evaluation

Recently, the concept of combining multiple classifiers has been actively exploited for developing highly reliable "diagnostic" systems [7]. One of the key issues of this approach is how to combine the results of the various systems to give the best estimate of the optimal result.

In this study, six subsystems have been developed, and each of them was associated with the six planes specified in the feature extraction process (*i.e. R, G, B, H, S, & V*). For each subsystem, 9 statistical features have been associated with, resulting thus a total 54 features space. Each subsystem was modelled with the proposed neurofuzzy learning scheme. This provides a degree of certainty for each classification based on the statistics for each plane. The outputs of each of these networks must then be combined to produce a total output for the system as a whole as can be seen in Fig. 4. While a usual scheme chooses one best subsystem from amongst the set of candidate subsystems based on a winner-takes-all strategy, the current proposed approach runs all multiple subsystems with an appropriate collective decision strategy. The aim in this study is to incorporate information from each plane/space so that decisions are based on the whole input space. The adopted in this paper methodology was to use the fuzzy integral concept. Fuzzy integral (FI) is a promising method that incorporates information from each space/plane so that decisions are based on the whole input space in the case of multiple classifier schemes. FI combines evidence of a classification with the systems expectation of the importance of that evidence.

By treating the classification results a series of disjointed subsets of the input space Sugeno defined the g_λ-fuzzy measure [8].

$$g(A \cup B) = g(A) + g(B) + \lambda g(A) g(B);$$
$$\lambda \in (-1, \infty) \tag{3}$$

where the λ measure can be given by solving the following non-linear equation.

$$\lambda + 1 = \prod_{i=1}^{K} (1 + \lambda g^i) \qquad \lambda > -1 \tag{4}$$

The g^i, $i \in \{1, ..., K\}$ values are fuzzy densities relating to the reliability of each of the K feature networks and satisfy the conditions of fuzzy sets laid out by Sugeno.

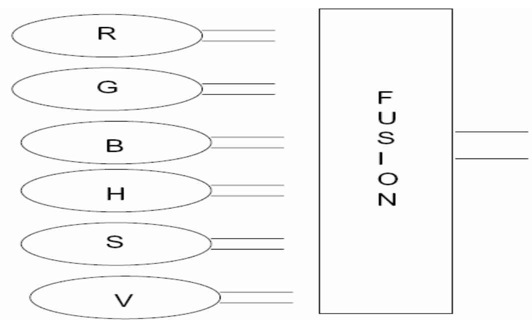

Fig. 4: Proposed fusion scheme and the neurofuzzy classifier

The classification scheme utilised here is an adaptive fuzzy logic system which utilises the gradient descent algorithm as a learning scheme.

A. Adaptive Fuzzy Logic System (AFLS)

The AFLS is one type of Fuzzy Logic System with a singleton fuzzifier and a defuzzifier. Its structure is the same as a normal FLS but its rules are derived and extracted from given training data. In other words, its parameters can be trained like a neural network approach, but with its structure in a fuzzy logic system structure. Since we have general ideas about the structure and effect of each rule, it is straightforward to effectively initialise each rule. This is a tremendous advantage of AFLS over its neural network counterpart. The centroid defuzzifier cannot be used because of its computation expense and that it prohibits using the back-propagation training algorithm. The proposed AFLS includes an alternative defuzzification approach, area of balance (AOB). This AFLS has the same approach as the system presented by Wang [9] and its feed-forward structure is shown in Fig. 5 with an extra "fuzzy basis" layer. The fuzzy basis layer consists of fuzzy basis nodes for each rule. A fuzzy basis node has the following form:

$$\phi_m(\bar{x}) = \frac{\mu_m(\bar{x})}{\sum_{l=1}^{L} \mu_l(\bar{x})} \tag{5}$$

where $\varphi_m(\bar{x})$ is a fuzzy basis node for rule *m* and $\mu_m(\bar{x})$ is a membership value of rule *m*. Since we use a product-inference, the fuzzy basis node $\mu_m(\bar{x})$ is in the following form:

$$\mu_m(\bar{x}) = \prod_{i=1}^{n} \mu_{F_i^m}(x_i) \tag{6}$$

where $\mu_{F_i^m}(x_i)$ is a membership value of the i^{th} input of rule *m*. In our case, a Gaussian shape as a membership function of each input of each rule has been used hence $\mu_{F_i^m}(x_i)$ will be in the following form:

$$\mu_{F_i^m}(x_i) = \exp\left[-\frac{(x_i - c_i^m)^2}{2(b_i^m)^2}\right] \tag{7}$$

where c_i^m and b_i^m are the centre and spread parameters, respectively, of the membership function i^{th} input of the m^{th} rule. The most popular defuzzification methods are the centroid of area (COA) and centre average (CA). The former although more accurate than the latter, is well known for its computational cost. Centroid calculation returns the centroid of the area formed by the consequent membership function, the membership value of its rules and the max-min or max- product inference.

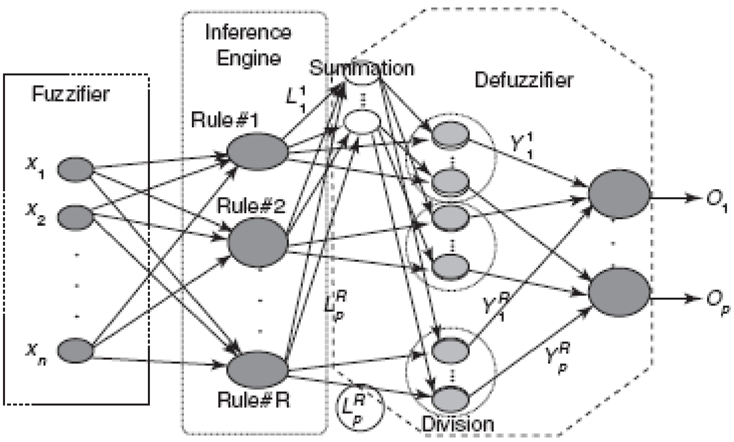

Fig. 5: Neurofuzzy classifier

However, since the COA method provides good performance, its main characteristics, centre of gravity and use of the shape of membership function, will be preserved in the design of the proposed defuzzification approach. The overall output of the system may be the result of fuzzy union or the addition of rule outputs as in Kosko's method. The proposed AFLS uses Kosko's method with product inference [10]. In general form, the calculation of the output, y, will be

$$y_p = \frac{\sum_{m=1}^{M} \mu_m L_p^m y_p^m}{\sum_{m=1}^{M} \mu_m L_p^m} \tag{8}$$

where y_p : the p^{th} output of the network, μ_m : the membership value of the m^{th} rule, L_p^m : the spread parameter of the membership function in the consequent part of the p^{th} output of the m^{th} rule, y_p^m : the centre of the membership function in the consequent part of the p^{th} output of the m^{th} rule.

The gradient descent learning (back-propagation) scheme has been used to update its various parameters. The update equations for y_p^m , L_p^m , c_i^m and b_i^m are:

$$y_p^m(n+1) = y_p^m(n) + m_y[y_p^m(n) - y_p^m(n-1)] - \eta_y \frac{\partial J}{\partial y_p^m}|_n \tag{9}$$

$$L_p^m(n+1) = L_p^m(n) + m_L[L_p^m(n) - L_p^m(n-1)] - \eta_L \frac{\partial J}{\partial L_p^m}|_n \tag{10}$$

$$c_i^m(n+1) = c_i^m(n) + m_c[c_i^m(n) - c_i^m(n-1)] - \eta_c \frac{\partial J}{\partial c_i^m}|_n \tag{11}$$

$$b_i^m(n+1) = b_i^m(n) + m_b[b_i^m(n) - b_i^m(n-1)] - \eta_b \frac{\partial J}{\partial b_i^m}|_n \tag{12}$$

where, J_k the objective function is defined as:

$$J_k = \frac{1}{2}\sum_{p=1}^{P}(y_p(\bar{x}_k) - d_p(\bar{x}_k))^2 \tag{13}$$

with P the number of outputs, d_p the desired response of the p^{th} output and $y_p(\bar{x}_k)$ defined as in Eq. 8.

IV. Results

The proposed approach was evaluated using 140 clinically obtained endoscopic M2A images. For the present analysis, two decision-classes are considered: abnormal and normal. Seventy images (35 abnormal and 35 normal) were used for the training and the remaining ones (35 abnormal and 35 normal) were used for testing. The extraction of quantitative parameters from these endoscopic images is based on texture information. Initially, this information is represented by a set of descriptive statistical features calculated on the histogram of the original image. In a second stage, the N_{TU}-based extraction process, the texture spectrum of the six components (*R, G, B, H, S, V*) have been obtained from the texture unit numbers, and the nine statistical measures have been used in order to extract new features from each textures spectrum. In this research study, both colour spaces (i.e. RGB and HSV) have been utilised. The adopted approach was based on the assumption that different colour spaces produce independent representations of the different colour texture patterns [14][15]. A multi classifier consisting of AFLS networks with 9 input nodes and 2 output nodes was trained on each of the six feature spaces.

A.Performance of Histograms-based features

The network trained on the R feature space achieved an accuracy of 92.85% on the testing data incorrectly classifying 3 of the normal images as abnormal and 2 abnormal as normal ones. The network trained on the G feature space misclassified 2 abnormal images as normal but not the same ones as the R space. The remaining one image was misclassified as normal ones. The B feature space achieved an accuracy of 94.28% on the testing data with 4 misclassifications, i.e. 2 abnormal as normal ones and the remaining two images as abnormal ones. The network trained on the H feature space achieved 94.28% accuracy on the testing data. The network trained on the S feature space achieved an accuracy of only 91.42% on the testing data. Finally, the network for the V feature space misclassified 2 normal cases as abnormal ones, giving it an accuracy of 97.14% on the testing data. The soft combination of neural classifiers using FI fusion concept resulted in 92.85% accuracy over the testing dataset (5 mistakes out of 70 testing patterns), demonstrating in this way the efficiency of this scheme in terms of accuracy. More specifically, 2 normal cases have been considered as abnormal while 3 abnormal as normal ones. The results, as shown in Fig. 6, indicate a high confidence levels for each correct classification, such as 0.63, while Table 1 presents the performance of individual components.

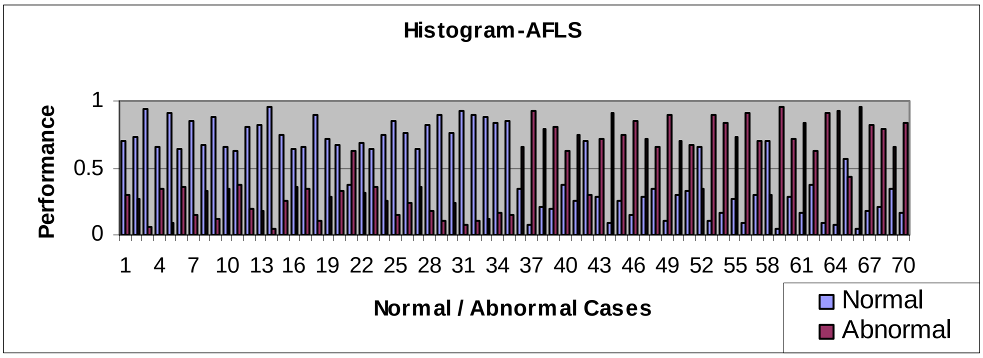

Fig. 6: AFLS with FI fusion for Histogram

B. *Performance of N_{TU}-based features*

In the N_{TU}-based extraction process, the texture spectrum of the six components (R, G, B, H, S, V) have been obtained from the texture unit numbers, and the same nine statistical measures have been used in order to extract new features from each textures spectrum. The AFLS network trained on the R feature space achieved an accuracy of 94.28% on the testing data incorrectly classifying 2 of the normal images as abnormal and 2 abnormal as normal ones. The network trained on the G feature space misclassified 3 normal images as abnormal but not the same ones as the R space. The B feature space achieved an accuracy of 97.14% on the testing data with 2 misclassifications, i.e. one abnormal as normal one and the remaining one image as abnormal one. The network trained on the H feature space achieved 97.14% accuracy on the testing data. The network trained on the S feature space achieved an accuracy of only 92.86% on the testing data. Finally, the network for the V feature space misclassified two normal cases as abnormal ones, giving it an accuracy of 97.14% on the testing data. The soft combination of AFLS classifiers using FI fusion concept resulted in

95.71% accuracy over the testing dataset (3 mistakes out of 70 testing patterns), demonstrating in this way again the efficiency of this scheme in terms of accuracy.

Table 1: AFLS Performances

Modules	Histogram Accuracy (70 testing patterns)	N_{TU} Accuracy (70 testing patterns)
R	92.85% (5 mistakes)	94.28% (4 mistakes)
G	95.71% (3 mistakes)	95.71% (3 mistakes)
B	94.28% (4 mistakes)	97.14% (2 mistakes)
H	94.28% (4 mistakes)	97.14% (2 mistakes)
S	91.42% (6 mistakes)	92.86% (5 mistakes)
V	97.14% (2 mistakes)	97.14% (2 mistakes)
Overall	92.85% (5 mistakes)	95.71% (3 mistakes)

More specifically, 2 normal cases as abnormal and one abnormal as normal one provide us a good indication of a "healthy" diagnostic performance [11]. However the level of confidence in this case was slight less than the previous case (i.e. the histogram), that is 0.59 as shown in Fig. 7.

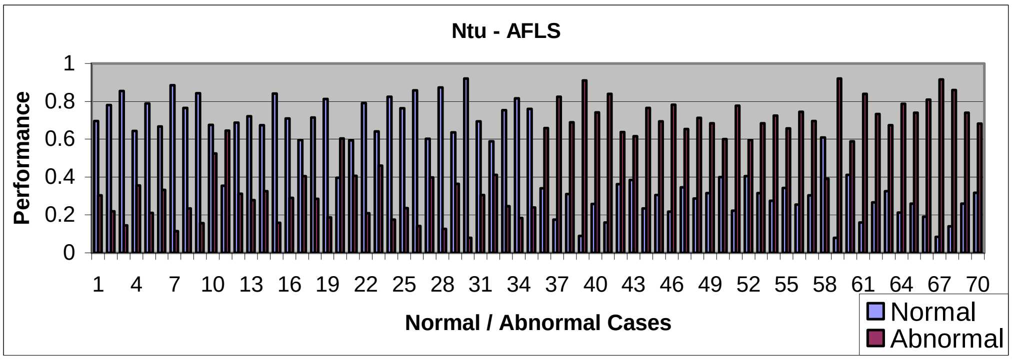

Fig. 7: AFLS with FI fusion for N_{TU}

The aim of this research study was to combine the diverse information contained in the two colour spaces and to improve thus texture discrimination. This approach provides the opportunity to exploit the strengths of different colour representations encapsulated by individual experts while avoiding their weaknesses, making the overall final decision more accurate [15]. The performance of the combined system (using the fuzzy integral concept) in terms of accuracy (i.e. correct diagnosis) was superior those of RGB and HSV colour spaces). This can be shown in Table 1. For example, in the N_{TU} case, both RGB and HSV have 9 incorrect cases each, where the overall system by applying the fuzzy integral achieved a greater performance with 3 incorrect cases. Thus the overall classification results were significantly improved by using this modular system (multi-space) approach.

However, medical diagnostic tests are often perceived by physicians as providing absolute answers or as clarifying uncertainty to a greater degree than is warranted. When a diagnosis turns out to be at variance with the results of a diagnostic test, the clinician's assumption may be that the test was either misinterpreted or that the test is no good. Such a binary approach to the interpretation of diagnostic testing, i.e., assuming a clearly positive or negative result (like an off-on switch), is too simplistic and may be counterproductive in the workup of a patient.

Instead, the results of a diagnostic test should be viewed on a continuum from negative to positive and as giving the likelihood or probability of a certain diagnosis. The performance of a neural network is usually expressed in terms of its estimation and prediction rates, that is, the number of correctly classified objects in the train and prediction sets, respectively. While these estimators may be adequate in certain instances, e.g., general classification tasks, they should not be employed when medical data is involved [12]. This is because such variables give only a measure of overall performance. In the case of human beings it is crucial to assess the capacity of a test to distinguish between people with (true positive) and without (true negative) a disease, as those individuals may or may not be subjected to further evaluations that may be stressing, costly, etc., depending upon the result of the test. In these cases, the sensitivity and the specificity are more adequate. The performance of all the classification tools evaluated in the present work was thus assessed in terms of these variables which are estimated according to [12]:

$$sensitivity = \frac{\sum true\ positive\ alarms}{\sum true\ positive\ alarms\ + \sum false\ negative\ alarms}$$

$$specificity = \frac{\sum true\ negative\ alarms}{\sum true\ negative\ alarms\ + \sum false\ positive\ alarms}$$

However, although sensitivity and specificity partially define the efficacy of a diagnostic test, they do not answer the clinical concern of whether a patient does or does not have a disease. These questions are addressed by calculating the predictive value of the test

$$predictability = \frac{\sum true\ positive\ alarms}{\sum true\ positive\ alarms\ + \sum false\ positive\ alarms}$$

The above methodologies were verified through the calculation of these parameters for the N_{TU} AFLS case, and are illustrated in Table 2.

Table 2: Performance indexes

N_{TU} **AFLS**	**R**	**G**	**B**	**H**	**S**	**V**	**Overall**
Sensitivity	0.9428	1	0.9714	1	0.914	1	***0.9714***
Specificity	0.9428	0.914	0.9714	0.9428	0.9428	0.9428	***0.9428***
Predictability	0.9428	0.921	0.9714	0.9459	0.9411	0.9459	***0.944***

According to literature in medical endoscopy, texture descriptors are calculated with all planes of the colour space (i.e. R, G, B for RGB), rather than choosing a specific plane for feature extraction [3] [14]. As it is illustrated in Table 2, the performance of the proposed multi-classifier in those indices provides indeed a very satisfactory result. In a future work, data-dimensionality principles for each classifier could be investigated in order to optimise their input vector.

V. Conclusion

The major contribution of the proposed system in the process of medical diagnosis is that it can provide additional information to physicians on the characterisation of the endoscopic images / tissues, by exploiting its textural characteristics, which are consequently used for the classification of the corresponding image regions as normal or abnormal. An approach on extracting statistical features from endoscopic images using the M2A Given Imaging capsule have been developed by obtaining those quantitative parameters from the texture spectra from the calculation the texture unit numbers (N_{TU}) over the histogram spectrum. In this study, an intelligent decision support system has been developed for endoscopic diagnosis based on a multiple-classifier scheme. This multiple-classifier approach using Fuzzy integral as a fusion method provided encouraging results. Although, the AFLS network provided evidence of its strength, future studies will be focused on further development of this "diagnostic" system by investigating algorithms for reduction of input dimensionality as well as the testing of this approach to the a new endoscopic capsule - IVP, which was developed via the IST a European research project.

This research work was supported by the "IVP- Intracorporeal Videoprobe", European Research Project, Contract no: IST-2001-35169.

References

[1] Y. Haga, M. Esashi, "Biomedical Microsystems for Minimally Invasive Diagnosis and Treatment", *Proc. of IEEE*, Vol. 92, 2004, pp. 98-114.
[2] S. Krishnan, P. Wang, C. Kugean, M. Tjoa, "Classification of endoscopic images based on texture and neural network", *Proc. 23rd Annual IEEE Int. Conf. in Engineering in Medicine and Biology,* Vol. 4, 2001, pp. 3691-3695.
[3] D.E. Maroulis, D.K. Iakovidis, S.A. Karkanis, D.A. Karras, "CoLD: a versatile detection system for colorectal lesions endoscopy video-frames", *Computer Methods and Programs in Biomedicine,* Vol. 70, 2003, pp. 151–166.
[4] G. Idden, G. Meran, A. Glukhovsky and P. Swain, "Wireless capsule endoscopy", *Nature*, 2000, pp. 405-417
[5] R.M. Haralick, "Statistical and structural approaches to texture", *IEEE Proc*., Vol. 67, 1979, pp. 786- 804
[6] M. Boulougoura, E. Wadge, V.S. Kodogiannis, H.S. Chowdrey, "Intelligent systems for computer-assisted clinical endoscopic image analysis", *2nd IASTED Int. Conf. on Biomedical Engineering, Innsbruck, Austria*, 2004, pp. 405-408.
[7] E. Wadge, V.S. Kodogiannis, "Intelligent diagnosis of UTI in vivo using gas sensor arrays", *Int. Conf. on Neural Networks and Expert Systems in Medicine and HealthCare, NNESMED 2003, Sheffield UK*, 2003, pp. 93-98.
[8] L.I. Kuncheva, *Fuzzy Classifier Design*, Physica-Verlag, 2000
[9] L.X. Wang, *Adaptive Fuzzy Systems and Control*, Prentice Hall, Inc, 1994.
[10] V.S. Kodogiannis, "An efficient fuzzy based technique for signal classification", *Journal of Intelligent & Fuzzy Systems*, Vol. 11, 2001, pp 65-84
[11] M. Boulougoura, *Computer-aided Diagnosis in Wireless-Capsule Endoscopy using Intelligent Systems*, MPhil Thesis, Westminster University, UK, 2005
[12] P. Szczepaniak, P. Lisboa, J. Kacprzyk, *Fuzzy Systems in Medicine*, Springer, 2000.
[13] C. Palm, "Color texture classification by integrative co-occurrence matrices", *Pattern Recognition*, Vol. 37, 2004, pp. 965-976
[14] S. Karkanis, D. Iakovidis, D. Maroulis, D. Karras, M. Tzivras, "Computer-Aided Tumor Detection in Endoscopic Video Using Color Wavelet Features", *IEEE Trans. on Information Technology in Biomedicine*, Vol. 7, No. 3, 2003, pp 141-152.
[15] S. Chindaro, K. Sirlantzis, F. Deravi, "Texture Classification System using Colour Space Fusion", *IEE Electronics Letters*, Vol.41, No.10, 2005, pp. 589-590.

Dr. Vassilis S. Kodogiannis was born in Heraklion, Greece at 1966. He received the Elec. Eng. Degree from University of Thrace in 1990, the MSc in VLSI Systems Eng. from UMIST, in 1991 and the PhD in Electrical Eng. from Liverpool University in 1994. He is currently Principal Lecturer in the School of Computer Science at Univ. of Westminster, London. His research interests are in the areas of Intelligent Systems, Control and Image Processing.

Maria G. Boulougoura was born in Athens, Greece, in 1978. She received the diploma degree in Elec. & Comp. Eng. from University of Thrace in 2002 and the MPhil in Computer Science from Univ. of Westminster in 2006. She worked as a Research Assistant for the "Intracorporeal Video Probe" European Research Project, Sept. 2002-Dec. 2004. She is currently working at IBM Hellas S.A, in Athens, Greece.